# Thermodynamic Stability Assessment of Oxides, Nitrides, and Carbides in Liquid Sn-25Li

S. Sharafat and N. Ghoniem

Mech. & Aerospace Engr. Dept.
University of California Los Angeles
Los Angeles, CA 90095-1597

APEX Study
University of California Los Angeles
August 2000

UCLA-UCMEP-00-32

# ABSTRACT

The APEX study has identified tin-lithium (Sn-25Li; 25 at. % Li) as a potential new liquid wall coolant for handling high wall loads. Compared with Pb-Li, tin has a lower density and lower vapor pressure. The vapor pressure of Sn is several orders of magnitude lower than that of pure lithium. The thermal conductivity of Sn-25Li is about 3 times that of Pb-17Li and only about 20% less compared with pure lithium. However, the breeding ratio of Sn-25Li is marginal relative to those of pure Li and Pb-17Li, which may necessitate additional multiplier material.

To address the critical issues of magnetohydrodynamic pressure drop, ceramic coatings on structural materials are being developed for liquid-metal cooled concepts. The compatibility of oxides, nitrides, and carbides with Sn-Li is of fundamental importance to assess the viability of Sn-Li as a coolant for fusion applications. Here we report the results of thermodynamic calculations of the chemical stability of insulating ceramic materials in liquid Sn-Li as a function of temperature and composition (lithium concentration $x_{Li}$).

Results of the thermodynamic analysis show that many non-metal structural materials, such as nitrides, carbides (including SiC) and some of the oxides may be stable in Sn-Li at elevated temperatures (< 900°C).

Owing to the lack of experimental data, such as, the solubility of solutes in liquid Sn-Li, several assumptions had to be made to complete the thermodynamic analysis. The results of the stability analysis are therefore not conclusive and are only meant to serve as guidelines for assessing the viability of Sn-Li as a coolant material for fusion applications.

# TABLE OF CONTENTS

# LIST OF FIGURES

# LIST OF TABLES

# 1. Introduction

The APEX study [1] has identified tin-lithium (Sn-25Li; 25 at. % Li) as a potential new liquid wall coolant for handling high wall loads. Compared with Pb-Li, tin has a lower density and lower vapor pressure. The vapor pressure of Sn is several orders of magnitude lower than that of pure lithium. The thermal conductivity of Sn-25Li is about 3 times that of Pb-17Li and only about 20% less compared with pure lithium. However, the breeding ratio of Sn-25Li is marginal relative to those of pure Li and Pb-17Li, which may necessitate additional multiplier material.

Table 1 and 2 list physical and thermal data of Sn, respectively. The thermo-physical and thermodynamic properties of liquid Sn and some of its compounds were summarized in a recent report [2]. Figure 1 shows the vapor pressure of Sn-Li, which is of fundamental importance to plasma performance for liquid wall concepts. The vapor pressure is dominated by lithium, thus for a Sn-25Li alloy, the allowable operating temperature of the Sn-Li coolant is about 200°C higher than for pure lithium. The higher allowable operating temperature can result in an increase of coolant exit temperature and therefore, thermal efficiency. Sn has a slightly higher electrical resistivity (see Fig. 2) compared with Li and therefore, magneto-hydro-dynamic (MHD) effects are important. The use of a ceramic coating may thus be necessary to minimize MHD effects.

Limited experimental data of static corrosion tests show that refractory metals and some of their alloys are compatible with liquid Sn up to 800°C. However, Ni-based and Fe-based alloys are not [3]. However, to address the critical issues of magnetohydrodynamic (MHD) pressure drop, ceramic coatings on structural materials are being developed for liquid-metal cooled concepts. The compatibility of oxides, nitrides, and carbides with Sn-Li is of fundamental importance to assess the viability of Sn-Li as a coolant for fusion applications. Here we report the results of thermodynamic calculations of the chemical stability of insulating materials in liquid Sn-Li as a function of temperature and composition ($x_{Li}$ concentration in Sn-Li). We considered a composition range between 10 and 90 at. % Li and a temperature range between 500°C and 1500°C.

First, the activity-temperature-composition relationship of lithium in Sn-Li was estimated. Next, thermodynamic calculations of dissolved solutes (O, C, H, and N) were performed to determine their chemical activity as a function of temperature and composition in saturated liquid Sn-Li. Using the activity of the solutes and the Gibbs free energy of formation of corresponding lithium salts ($Li_2O$, LiH, $Li_3N$, and $Li_2C_2$) the stability region of these salts was mapped out as a function of temperature and composition. Finally, the stability of ceramic materials in Sn-25Li at 773°K was estimated using the Gibb's free energy data of various oxide, nitride, and carbide ceramic materials.

**Table 1: Physical Properties of Tin [4].**

| | | |
|---|---|---|
| *Density* | | |
| α-Tin | measured at 288K | 7.29 g $cm^{-3}$ |
| β-Tin | measured at 288K | 5.77 g $cm^{-3}$ |
| *Liquid* | measured at m.p. | 6.968±0.005 g $cm^{-3}$ |
| | measured at 600 K | 6.70 g $cm^{-3}$ |
| | measured at 1200K | 6.29 g $cm^{-3}$ |
| *Hardness* | *(Moh scale)* | 1.5 –1.8 |
| | at 293 K | 3.9 HB |
| | at 373 K | 2.3 HB |
| | at 473 K | 0.9 HB |
| *Resistivity* | | |
| α-Tin | measured at 293K | 12.6 μΩ cm |
| β-Tin | measured at 273K | 300 μΩ cm |
| *Young's modulus (at 293 K)* | | 49.9 kN $mm^{-2}$ |
| *Bulk modulus (at 293 K)* | | 58.2 kN $mm^{-2}$ |
| *Shear strength (at RM)* | | 12.3 N $mm^{-2}$ |

**Table 2: Thermal Data of Tin [4].**

| | |
|---|---|
| Fusion point | 231.9681 °C |
| Enthalpy of fusion | 7.06 kJ g atom$^{-1}$ |
| Boiling point | 2270°C |
| Enthalpy of vaporization | 296.4 kJ g atom$^{-1}$ |
| Vapor pressure | |
| at 1096 K | $10^{-5}$ mm Hg |
| at 1196 K | $10^{-4}$ mm Hg |
| at 1315 K | $10^{-3}$ mm Hg |
| at 1462 K | $10^{-2}$ mm Hg |
| at 1646 K | $10^{-1}$ mm Hg |
| at 1882 K | 1 mm Hg |
| Specific heat ($C_v$) at 298 K | |
| $\alpha$-Tin | 215.5 J kg$^{-1}$ K$^{-1}$ |
| $\beta$-Tin | 223.3 J kg$^{-1}$ K$^{-1}$ |
| Thermal conductivity at 273.2 K | |
| Polycrystalline | 0.682 W cm$^{-1}$ K$^{-1}$ |
| Coefficient of expansion at 273 K | |
| Linear | $19.9 \times 10^{6}$ |
| Cubical | $59.8 \times 10^{6}$ |
| Expansion on melting | 2.3 % |
| Surface tension at melting point | 544 mN m$^{-1}$ |
| Viscosity at melting point | 1.85 mNs m$^{-2}$ |
| Gas solubility in liquid tin | |
| oxygen at 809 K | 0.00018% |
| oxygen at 1023 K | 0.0049% |
| hydrogen at 1273 K | 0.04% |
| hydrogen at 1573 K | 0.36% |

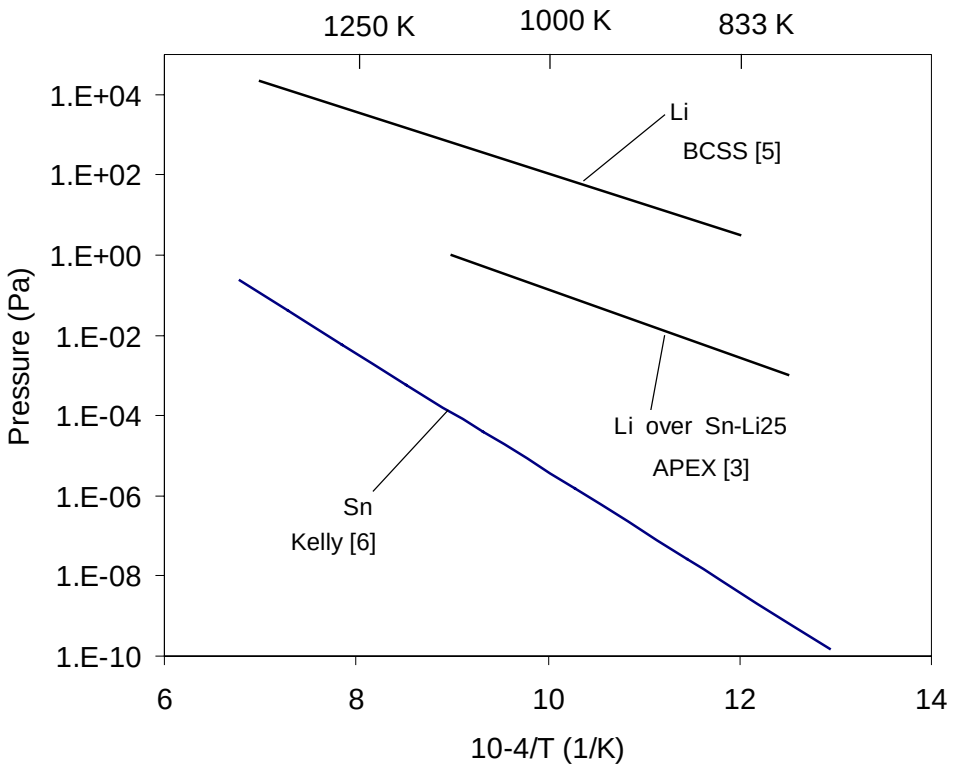


**Figure 1: Comparison between the vapor pressures of liquid coolants.**

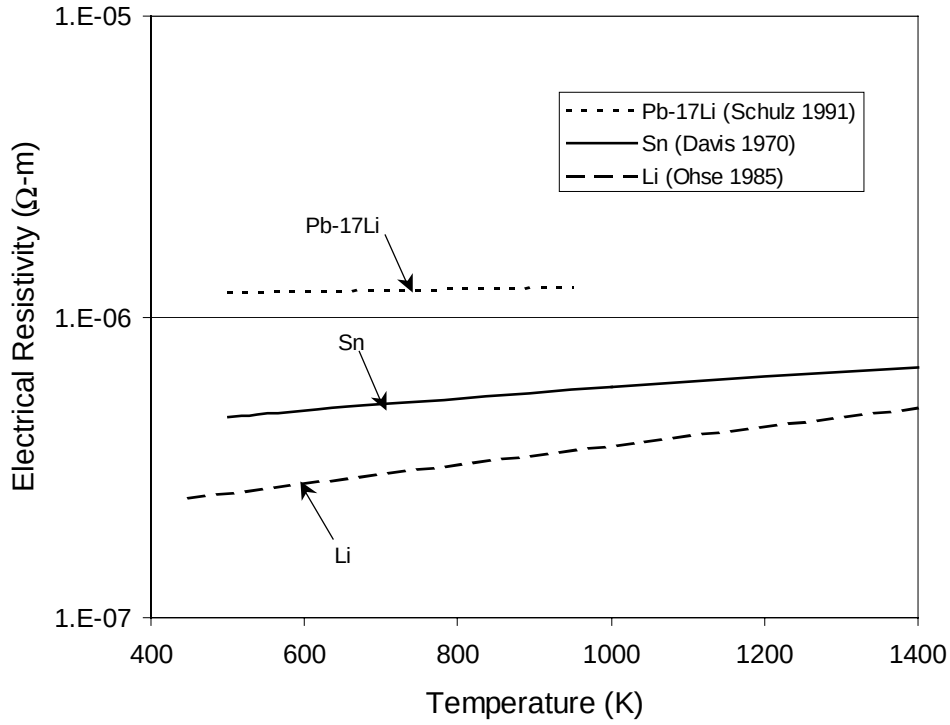


**Figure 2: Electrical resistivity of liquid Sn, Pb-17Li, and Li.**

## 2. Sn-Li Phase Diagram

Based on the Li-Sn phase diagram (Fig. 3) the minimum operating temperature for the Sn-25Li is about 330°C [10] to avoid the formation of the solid intermetallic compound $Li_2Sn_5$. Recently Natesan [11] fabricated a Sn-25 at.% Li alloy from pure Sn and Li. They measured the melting temperature of the alloy to be 334°C and its density to be 6.36 g/cm$^3$.

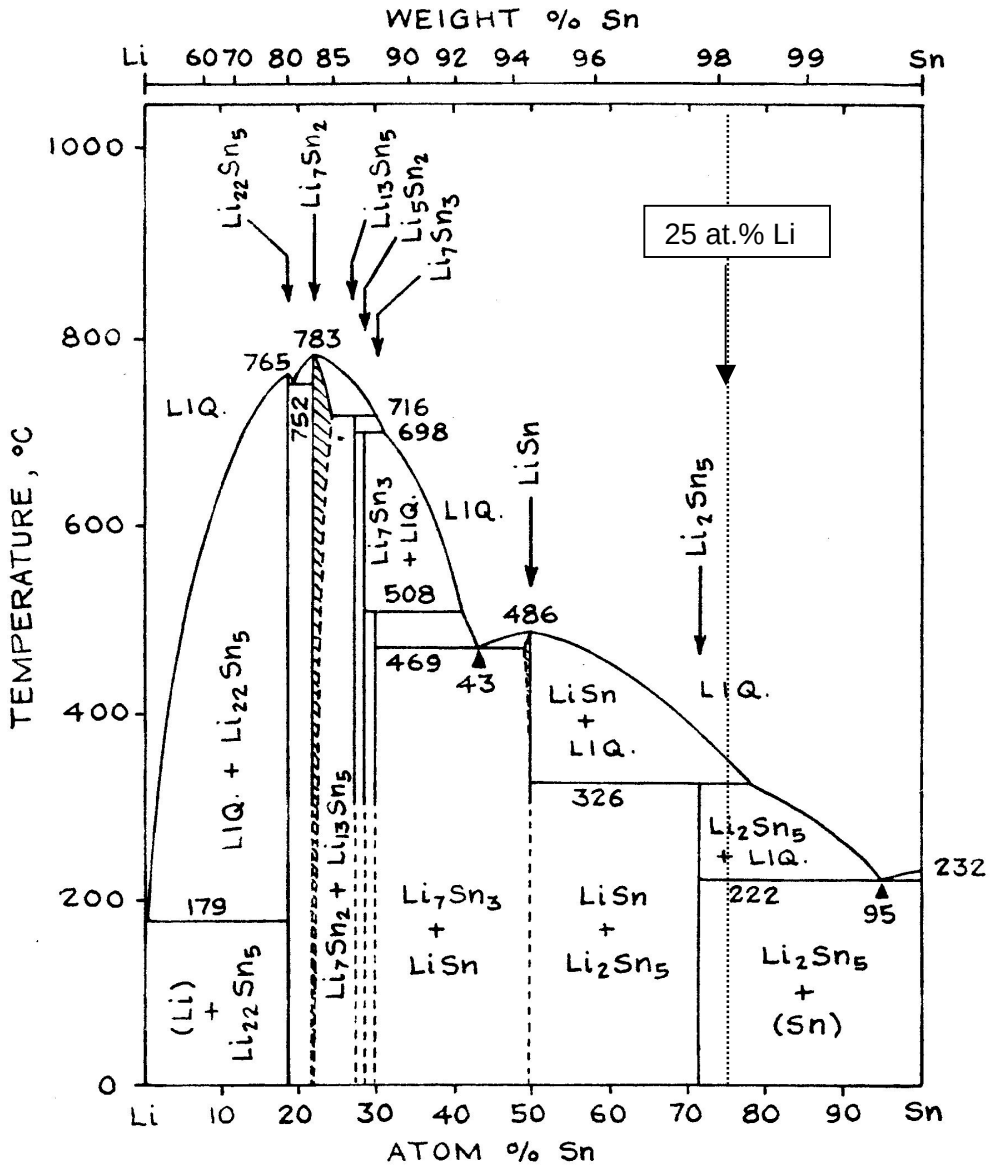


**Figure 3: Phase diagram of Li-Sn (after [10]).**

## 3. Chemical Activity of Li in Sn-Li

The activity of Li and Sn in Sn-Li was measured as a function of lithium concentration at 1200°C (see Table 3) and was reported by D. Sze [3].

**Table 3: Measured chemical activity of Li and Sn in Sn-Li at 1200°C (after [3]).**

| Li (at.%) | Li-Activity | Sn-Activity |
|---|---|---|
| 0.1 | 0.001 | 0.895 |
| 0.2 | 0.003 | 0.758 |
| 0.3 | 0.010 | 0.486 |
| 0.4 | 0.020 | 0.332 |
| 0.5 | 0.038 | 0.194 |
| 0.6 | 0.078 | 0.078 |
| 0.7 | 0.186 | 0.0155 |
| 0.8 | 0.354 | 0.00216 |
| 0.9 | 0.739 | 2.57E-05 |

Table 3 shows that the activity of both Li and Sn are very low, which are representative of similarly low activities of Li and Pb in the Pb-Li system [12,13]. To assess the stability of compounds in Sn-Li we need to know the activity of Li and Sn as a function of temperature. The activity-temperature relationship can be expressed as:

$$\ln a_{Li} = A + B/T \qquad (1)$$

The coefficients A and B need to be determined. Based on the activity data of Table 3, the composition-based ($x_{Li}$) activity relationship for Li at 1200°C can be approximated as:

$$\ln a_{Li} = -8.1442 + 14.097\, x_{Li} - 11.371\, x_{Li}^2 + 6.0259\, x_{Li}^3 \qquad (2)$$

The activity-temperature ($1.0 > x_{Li} > 0.1$) relationships for Pb-Li alloys for a temperature ranges between 523 K and 1023 K were reported by Hubberstey et al. [13]. Due to lack of data of the Sn-Li system, we use the Pb-Li system to estimate as a first approximation the coefficients in equation 1 for the Sn-Li system. Table 4 shows the estimated coefficients for the activity-temperature ($1.0 > x_{Li} > 0.1$) relationships for Li in Sn-Li alloys for a temperature ranges between 523 K and 1023 K. Thus, as a first approximation the activity-temperature relationship of Li in Sn-Li (eq. 1) has been formulated. However, these results should be used with caution, until experimental data for the activities of Li become available at various temperatures and compositions.

The activity-temperature relationship is shown in Fig. 4. The activity-temperature relationship shows that the Li activity decreases with decreasing Li fraction and with decreasing temperature.

**Table 4: Activity-temperature relationships for Pb-Li and Sn-Li alloys, ln $a_{Li}$ = A + B(T/K)$^{-1}$ (Pb-Li data after[13]).**

| $x_{Li}$ | A | B (Pb-Li) | B(Sn-Li) | Temperature (K) |
|---|---|---|---|---|
| 0.1 | -0.522 | -7071 | 769 | 523-1023 |
| 0.2 | -0.151 | -6624 | 222 | 523-1023 |
| 0.3 | 0.415 | -6378 | -611 | 613-1023 |
| 0.4 | 1.058 | -6209 | -1558 | 698-1023 |
| 0.5 | 1.652 | -5996 | -2433 | 755-1023 |
| 0.6 | 2.109 | -5618 | -3107 | 743-1023 |
| 0.7 | 2.284 | -4951 | -3364 | 915-1023 |
| 0.8 | 2.068 | -3874 | -3046 | 983-1023 |
| 0.9 | 1.346 | -2264 | -1983 | 823-1023 |

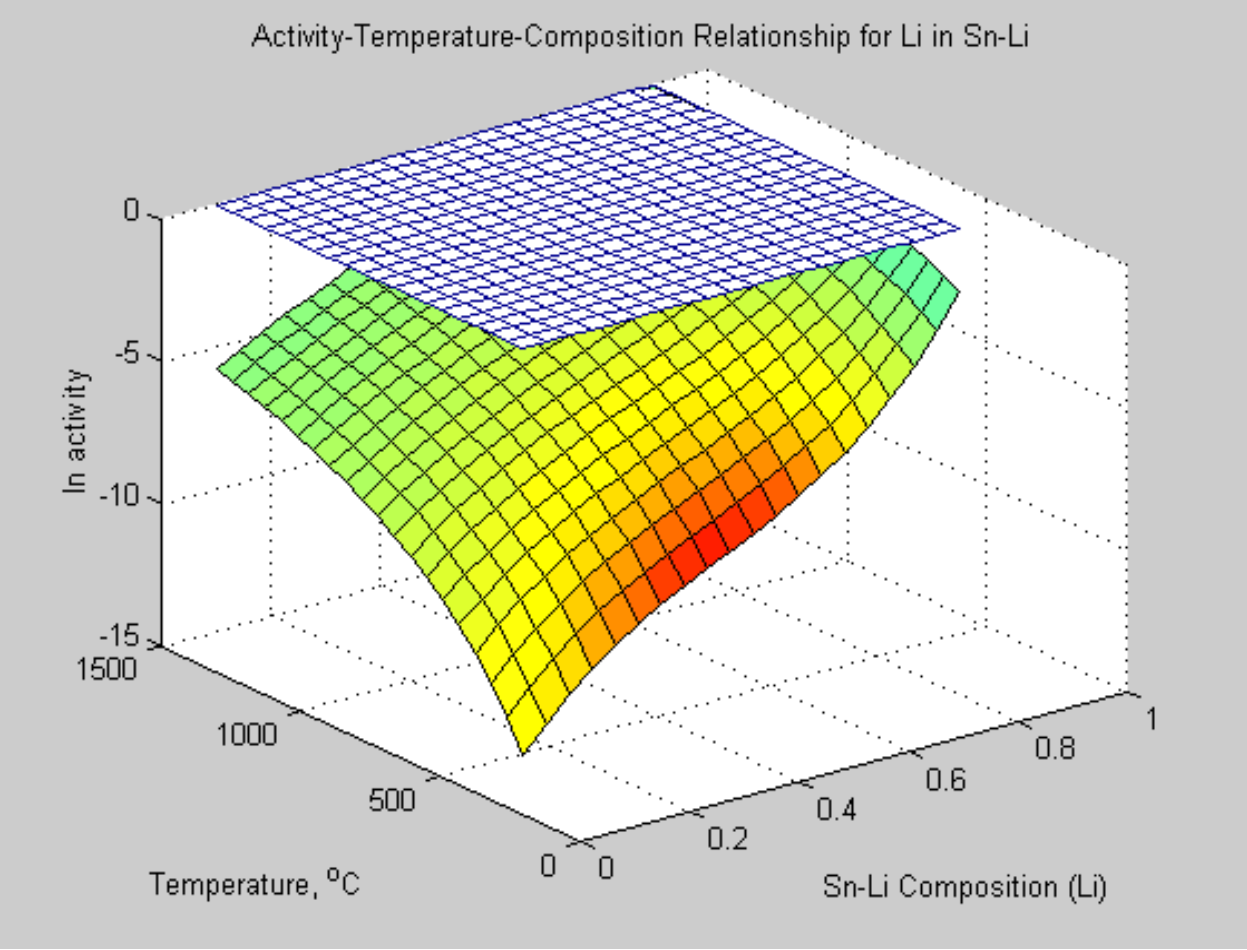


**Figure 4: Activity-Temperature-Composition Relationship for Li in Sn-Li.**

# 4. Thermodynamics of Dissolved Solutes in Sn-Li

The compatibility of ceramics with Sn-Li will depend on their thermodynamic stability ($\Delta_r G$, free energy of reaction) as a function of temperature, lithium concentration, and non-metal solute concentration. To evaluate $\Delta_r G$, the activity of the solutes, O, C, N, and H has to be known, which depend on the standard free energy of formation, $\Delta_f G$, of the corresponding Li-salts ($Li_2O$, $Li_3N$, $Li_2C_2$, and LiH). We show here the results of thermodynamics of the dissolved solutes (O, N, C, and H) as a function of temperature and composition.

### *4. 1 Activity of Solutes*

The activity relationships for oxygen, nitrogen, carbon, and hydrogen in Sn-Li can be calculated using equilibrium conditions of saturated solutions. We give here the representative equations for $Li_2O$, with similar expressions holding true for the other three salts considered ($Li_3N$, $Li_2C_2$, LiH):

$$2\,Li\,(Sn-Li)+O(Sn-Li) \overset{\Delta_f G^o(Li_2O)}{\rightleftarrows} Li_2O \qquad (3)$$

where, $\Delta_f G$ is evaluated at temperature *T* as:

$$\Delta_f G^\circ(Li_2O) = RT \ln K_e = RT \ln \{ a_{Li_2O} / a_{Li}^2 \cdot a_O \} \qquad (4)$$

where, *R* is the gas constant, $a_i$ is chemical activity of specie *i* and $K_e$ is the equilibrium constant, expressed by the RHS of eq. 4. The activity of $Li_2O$ is very low, thus equation 4 can be solved for the activity of the oxygen:

$$\ln a_O = \{ -\Delta_f G^\circ(Li_2O)/RT \} - 2 \ln a_{Li} \qquad (5)$$

The standard energy of formation of the salts, $Li_2O$, $Li_3N$, $Li_2C_2$, and LiH are given in the JANAF Thermochemcial Tables [14]. Table 5 lists the energy of formation of the salts with Table 6 giving the corresponding polynomials.

**Table 5: Standard free energy of formation ($\Delta_f G$) of some Li-salts ($Li_2O$, LiH, $Li_3N$, and $Li_2C_2$) [14].**

| | ΔG of Formation* (kJ/mol) | | | |
|---|---|---|---|---|
| Temp (K) | Li2O | LiH | Li3N | Li2C2 |
| 100 | -592.392 | -81.828 | -150.597 | |
| 200 | -584.794 | -75.511 | -140.16 | |
| 300 | -561.875 | -68.309 | -128.417 | -66.538 |
| 400 | -549.456 | -60.718 | -116.192 | -69.576 |
| 500 | -536.272 | -52.628 | -102.781 | -73.493 |
| 600 | -522.248 | -44.103 | -88.148 | -78.066 |
| 700 | -508.198 | -35.611 | -73.556 | -83.528 |
| 800 | -494.187 | -27.233 | -59.146 | -89.782 |
| 900 | -480.247 | -19.023 | -45.008 | -96.745 |
| 1000 | -466.401 | -11.022 | -31.203 | -104.35 |
| 1100 | -452.666 | -3.261 | -17.779 | -112.542 |
| 1200 | -439.054 | 4.233 | -4.769 | -121.775 |
| 1300 | -425.574 | 11.441 | 7.799 | -130.513 |
| 1400 | -412.23 | 18.345 | | -140.225 |
| 1500 | -399.026 | 24.929 | | -150.382 |
| 1600 | -385.961 | | | -160.962 |
| 1700 | -358.681 | | | -164.769 |
| 1800 | -328.002 | | | -167.192 |
| 1900 | -297.541 | | | -170.025 |
| 2000 | -267.29 | | | -173.252 |
| | | | | |
| "JANAF Thermochemcial Tables," J. Phys. Chem. Ref. Data, Vol. 14, Suppl. 1, 1985 | | | | |

**Table 6: Polynomial expressions for the standard free energy of formation of Li-salts as a function of temperature.**

| Salt | $\Delta_f G$ (kJ/mol) | Temp. (K) |
|---|---|---|
| $Li_2O$ | $5.109\times10^{-8} \times T^3 - 1.286\times10^{-4}\times T^2 + 2.282 \times10^{-1} \times T - 6.208\times10^{2}$ | 100-2000 |
| LiH | $-1.474\times10^{-8} \times T^3 + 3.285\times10^{-5} \times T^2 + 5.922 \times10^{-2} \times T - 8.841 \times10^{1}$ | 100-1500 |
| $Li_3N$ | $-3.549\times10^{-8} \times T^3 + 8.109\times10^{-5} \times T^2 + 8.320 \times10^{-2} \times T - 1.598 \times10^{2}$ | 100-1300 |
| $Li_2C_2$ | $4.026\times10^{-8} \times T^3 - 1.419\times0^{-4} \times T^2 + 7.573 \times10^{-2} \times T - 7.956 \times10^{1}$ | 300-2000 |

The chemical activities of Li, O, C, N, and H in Sn-Li at 773°K are shown in Fig. 5. It has been well known that most oxides are unstable in liquid lithium due to the stability of $Li_2O$ indicated by its large negative formation energy ($\Delta_f G^\circ(Li_2O)$ = -497.3 at 773°K). Figure 5 shows a strong negative activity of oxygen in Sn-Li for all values of $x_{Li}$. In contrast, for $x_{Li}$ below 0.6 the activity of C, N, and H are positive. It is therefore expected that carbide and nitride-based ceramics should be relatively stable in Sn-Li at 773°K and that LiH formation is suppressed at 773°K.

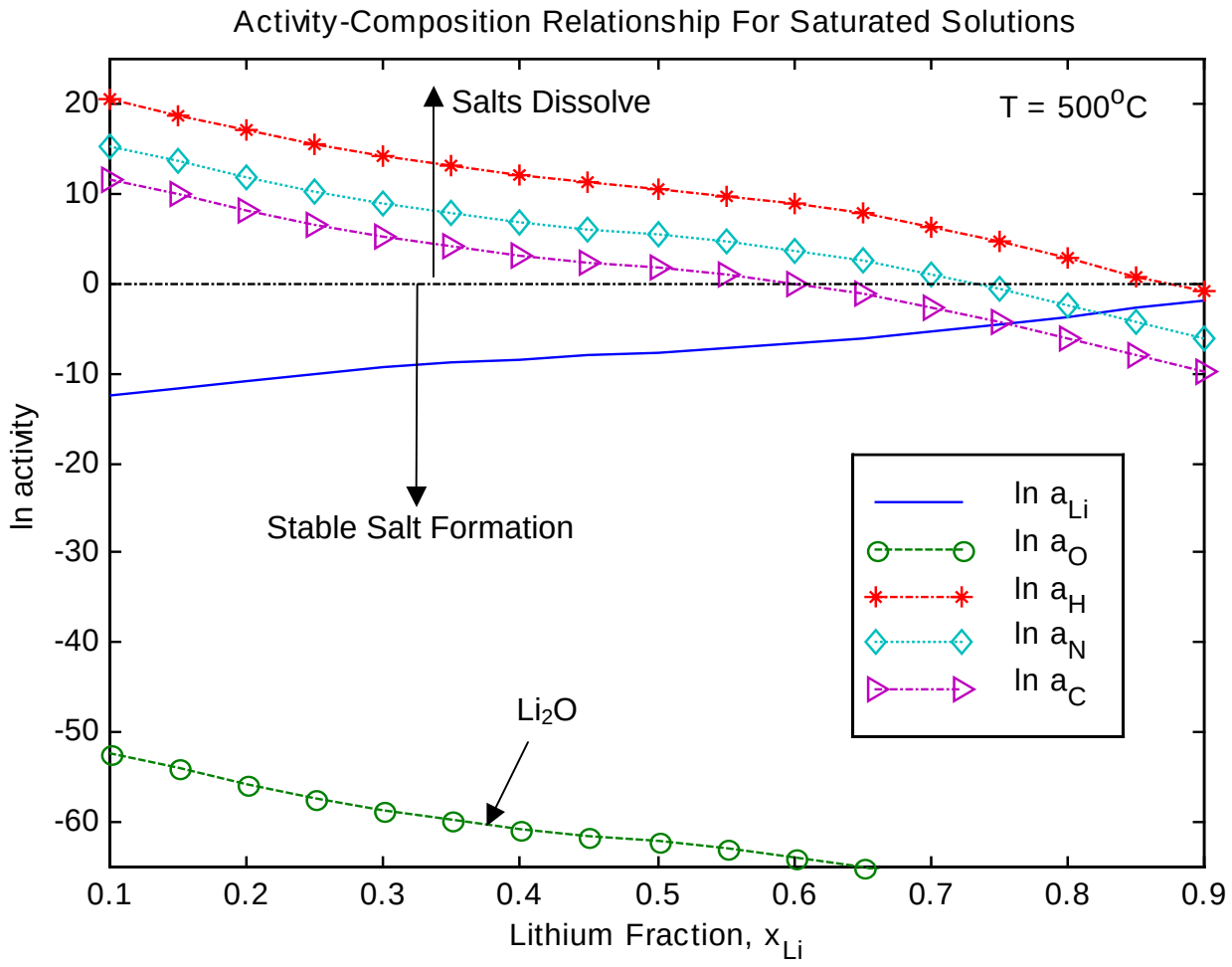


**Figure 5: Activity of Li, O, H, N, and C in saturated Sn-Li solutions as a function of composition at 773°K.**

Figure 6 shows the activities of Li, O, C, N, and H in saturated Sn-Li solution as a function of lithium composition ($x_{Li}$) at 1273°K. The activity of O, N, and H increase with temperature, while that of C drops slightly. In fact, formation of $Li_2C_2$ occurs at a lower Li composition ($x_{Li}$ = 0.5) at 1000°C compared with a composition of 0.6 at 500°C.

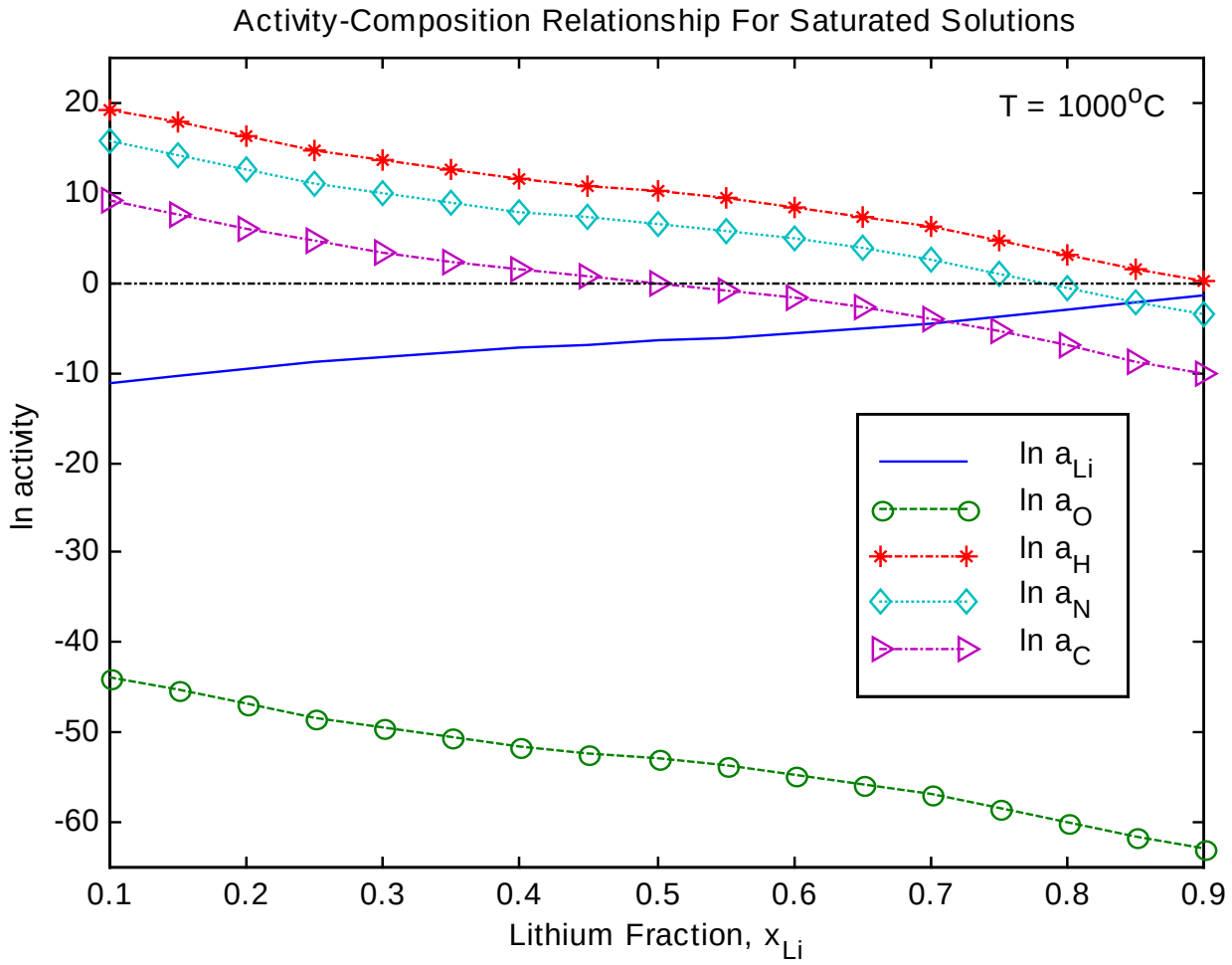


**Figure 6: Activity of Li, O, H, N, and C in saturated Sn-Li solutions as a function of composition at 1273°K.**

### 4. 1. 1 Activity of Oxygen

The activity relationship of oxygen in liquid Sn-Li as a function of temperature and $x_{Li}$, given by eq. 5, is shown in Fig 7.

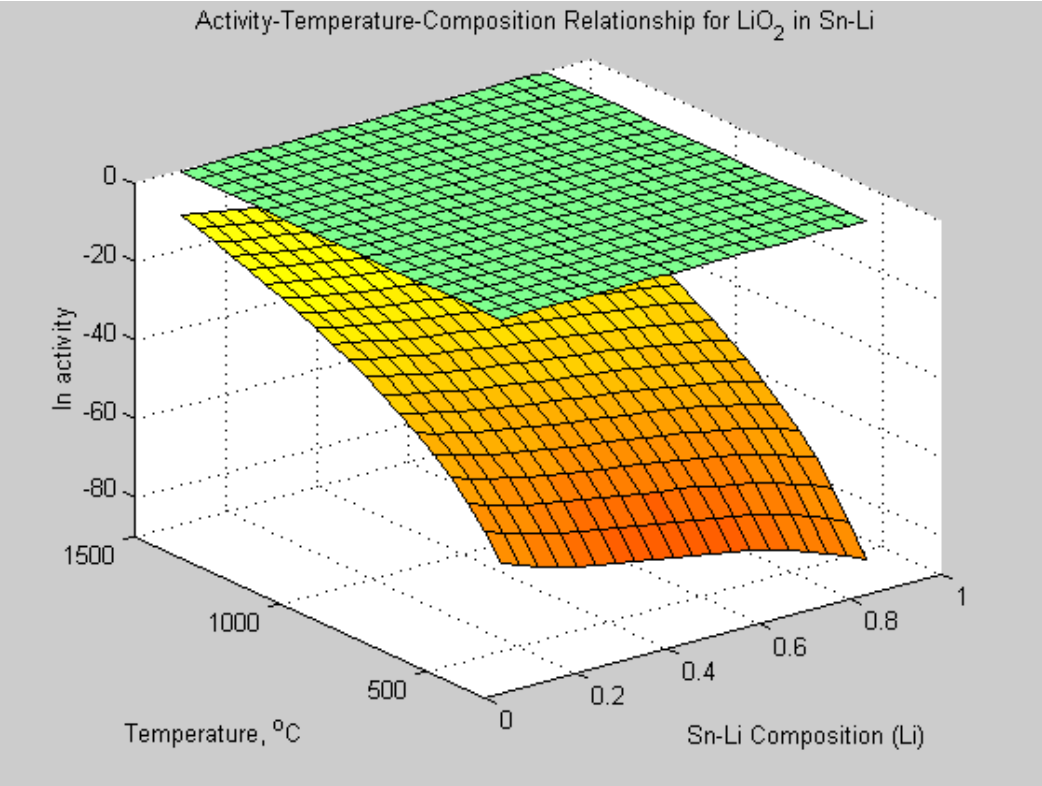


**Figure 7: Chemical activity of oxygen in Sn-Li in a saturated soltuion.**

The activity of oxygen in Sn-Li decreases with increasing temperatures for all combinations. However, the activity remains negative even at 1500°C. This indicates that $Li_2O$ is highly stable in Sn-Li and does not dissolve even at elevated temperatures.

### 4. 1. 2 Activity of Carbon

Figure 8 shows the activity relationship of carbon in liquid Sn-Li as a function of temperature and composition, $x_{Li}$. The activity of carbon changes from negative to positive values with decreasing $x_{Li}$ and increasing temperature. To clearer display the changeover region of $Li_2C_2$ formation, the temperature-composition phase space of $Li_2C_2$ activity is shown in Fig. 9. As the temperature increases, the lithium content needs to be decreased in order to avoid formation of $Li_2C_2$. Suppression of $Li_2C_2$ formation indicates a region of compatibility of carbide coatings in Sn-Li. The equation describing the composition-temperature activity relationship for carbon is given by:

$$ln\ a_C = \{-\Delta_f G^\circ(Li_2C_2)/RT\} - 2\ ln\ a_{Li} \qquad (6)$$

where $ln\ a_{Li}$ is given by equation 2.

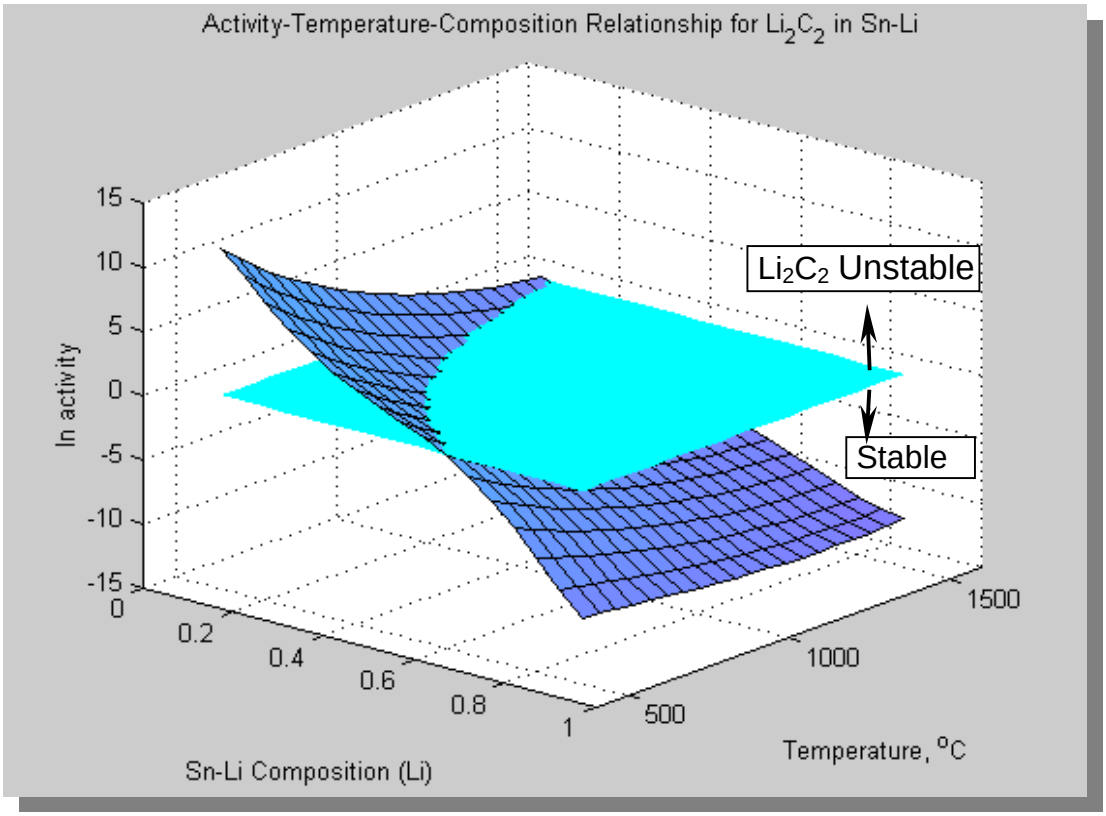


**Figure 8: Chemical activity of carbon in a saturated Sn-Li solution.**

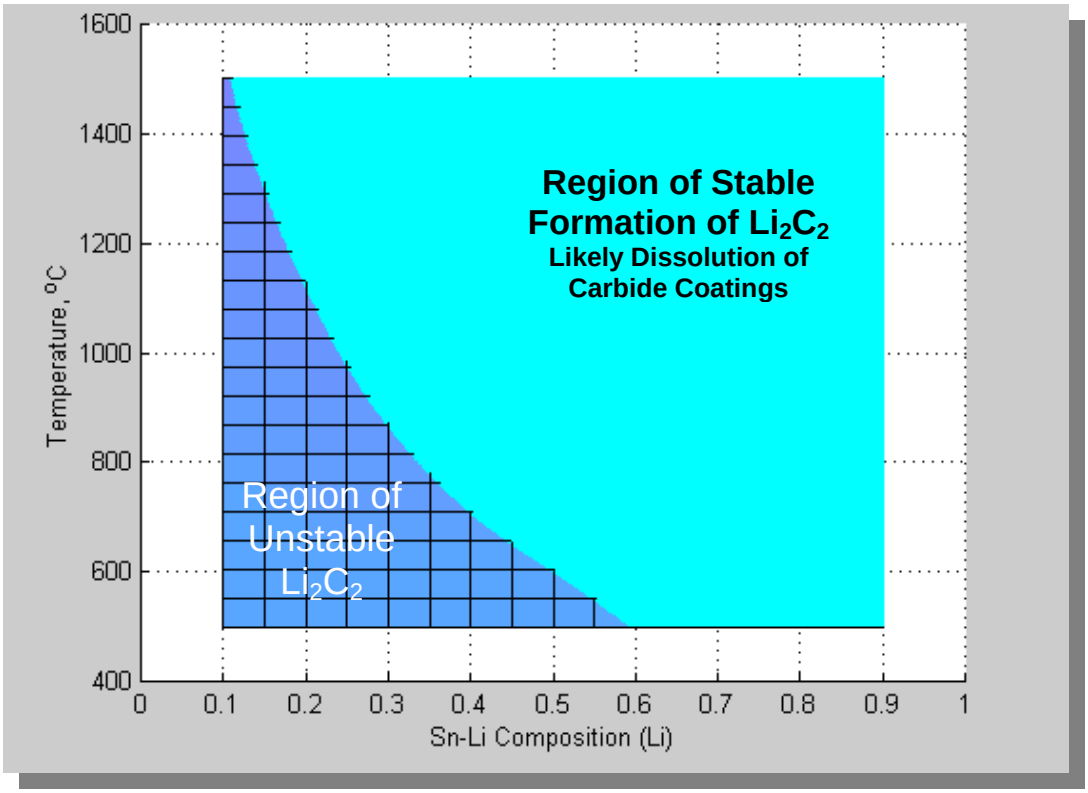


**Figure 9: Chemical activity of carbon in saturated Sn-Li solution (2-d representation of Fig. 8, showing $Li_2C_2$ stability limits in temperature-composition space).**

### 4. 1. 3 Activity of Nitrogen and Hydrogen

The activity relationship of nitrogen in saturated solution of Sn-Li as a function of temperature and $x_{Li}$ is shown in Fig. 10. The activity of nitrogen is positive activity for $x_{Li}$ above 0.75 at 500°C, which indicates that $Li_3N$ is unstable and will dissolve. At temperatures above 500°C the allowable Li content can be further increased. The small changeover region from stable to unstable $Li_3N$ formation is shown in the temperature-composition phase space of the $Li_3N$ of Fig. 11.

The equation describing the composition-temperature activity relationship for nitrogen is given by:

$$ln\ a_N = \{-\Delta_f G^\circ(Li_3N)/RT\} - 2\ ln\ a_{Li} \qquad (7)$$

where $ln\ a_{Li}$ is given by equation 2.

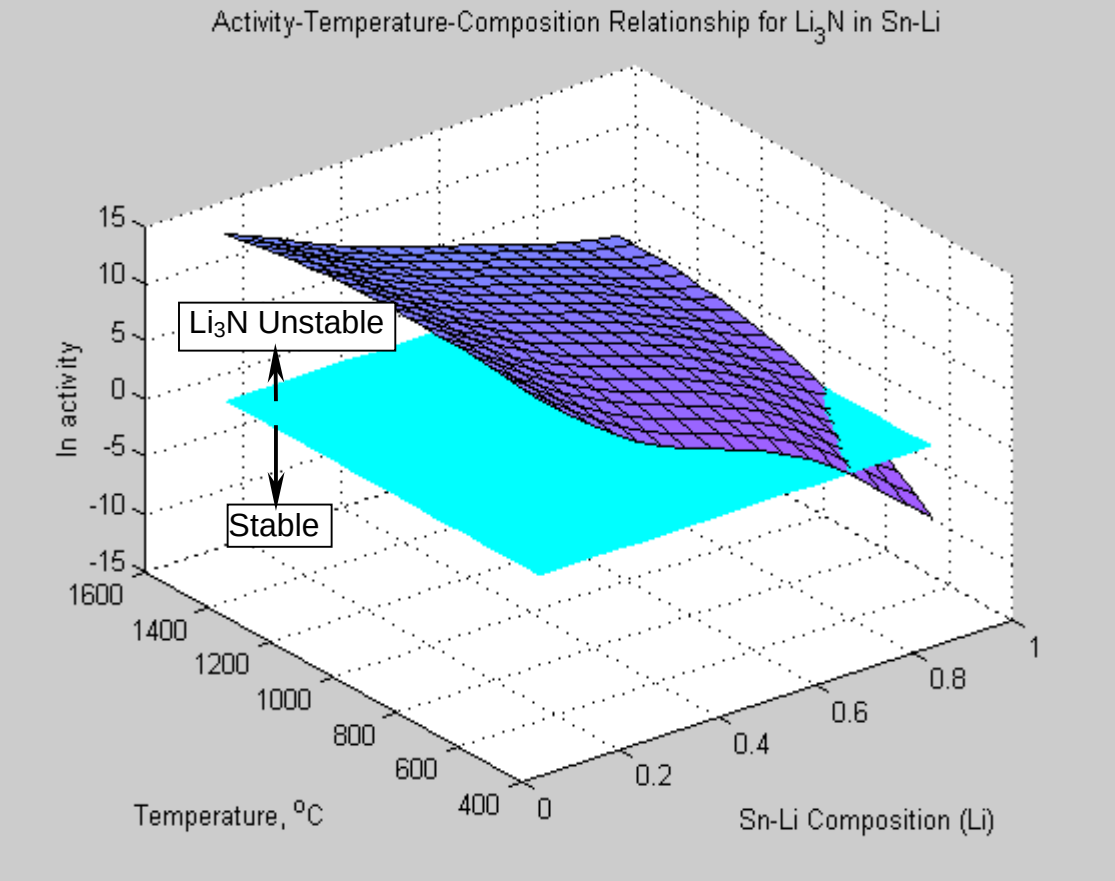


**Figure 10: Activity relationship for nitrogen in saturated Sn-Li solution.**

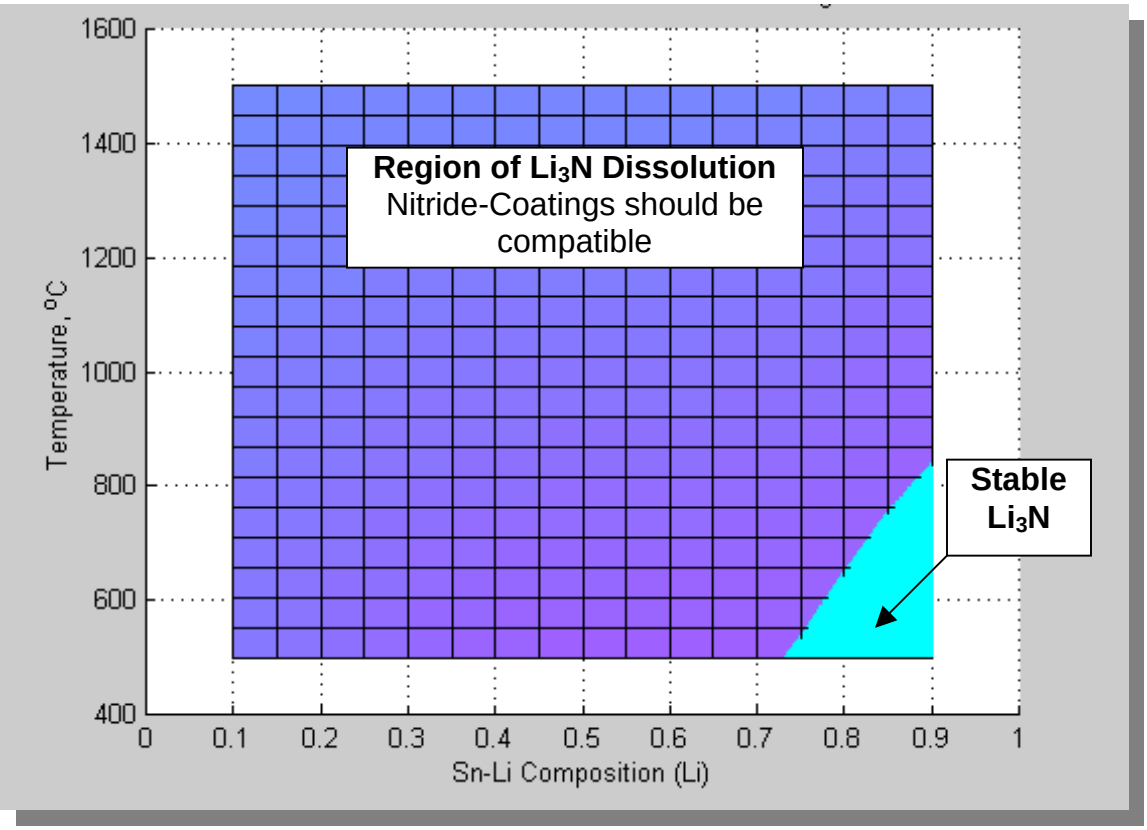


**Figure 11: Chemical activity of nitrogen in saturated Sn-Li solution (2-d representation of Fig. 10, showing the $Li_3N$ stability temperature-composition phase space).**

Figure 12 shows the stability volumes of hydrogen in saturated solution of Sn-Li as a function of temperature and composition. LiH formation is suppressed for almost all temperatures above 500°C and for all combinations. This indicates that tritium recovery from Sn-Li does not require handling of LiH salts.

The equation describing the composition-temperature activity relationship for hydrogen is given by:

$$ln\ a_H = \{-\Delta_f G^\circ(Li_H)/RT\} - 2\ ln\ a_{Li} \qquad (8)$$

where $ln\ a_{Li}$ is given by equation 2.

Figure 14 shows the limits of formation as defined by $ln\ a_i$ being zero, *i* being C, N, or H. ; The arrows in Fig. 14 indicated the corresponding sign of activities for each curve. The left hand side of each curve (positive activity) indicates dissolution of salts and the right hand side of each curve (negative activity) indicates stable lithium salt formation. Based on these results, LiH and Li3N will not precipitate from a Sn-25Li solution and $Li_2C_2$ will only do so for temperatures above 900°C.

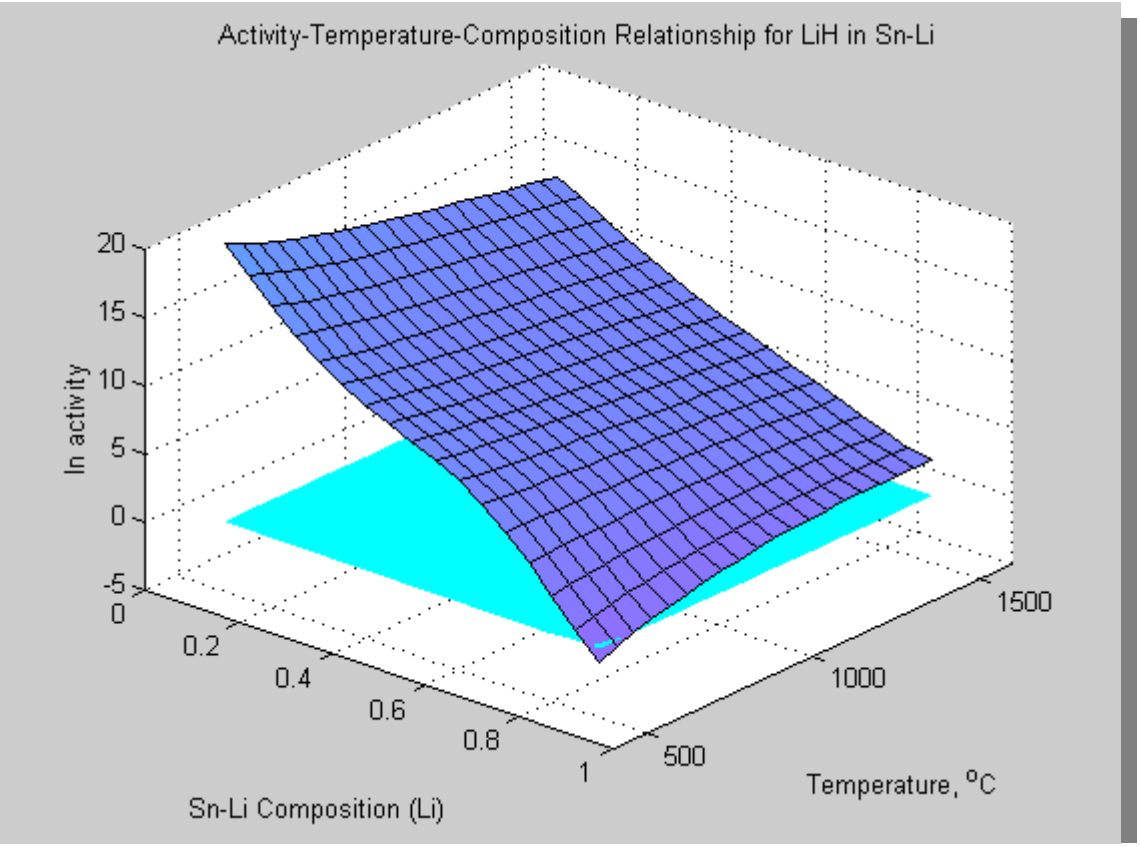


**Figure 12: Activity relationship for hydrogen in saturated solution of Sn-Li as a function of composition and temperature.**

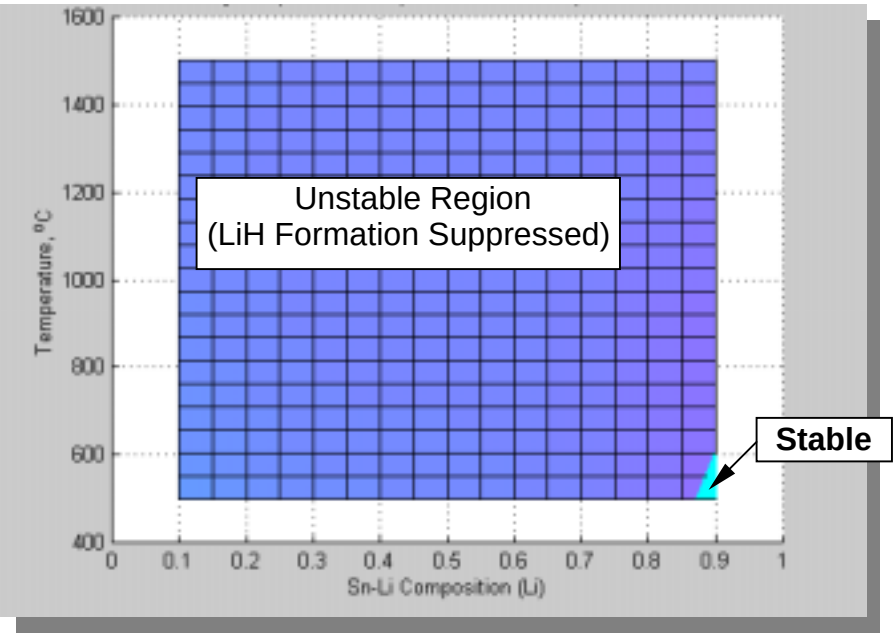


**Figure 13: Chemical activity of hydrogen in saturated Sn-Li solution (2-d representation of Fig. 12, showing the LiH stability temperature-composition phase space).**

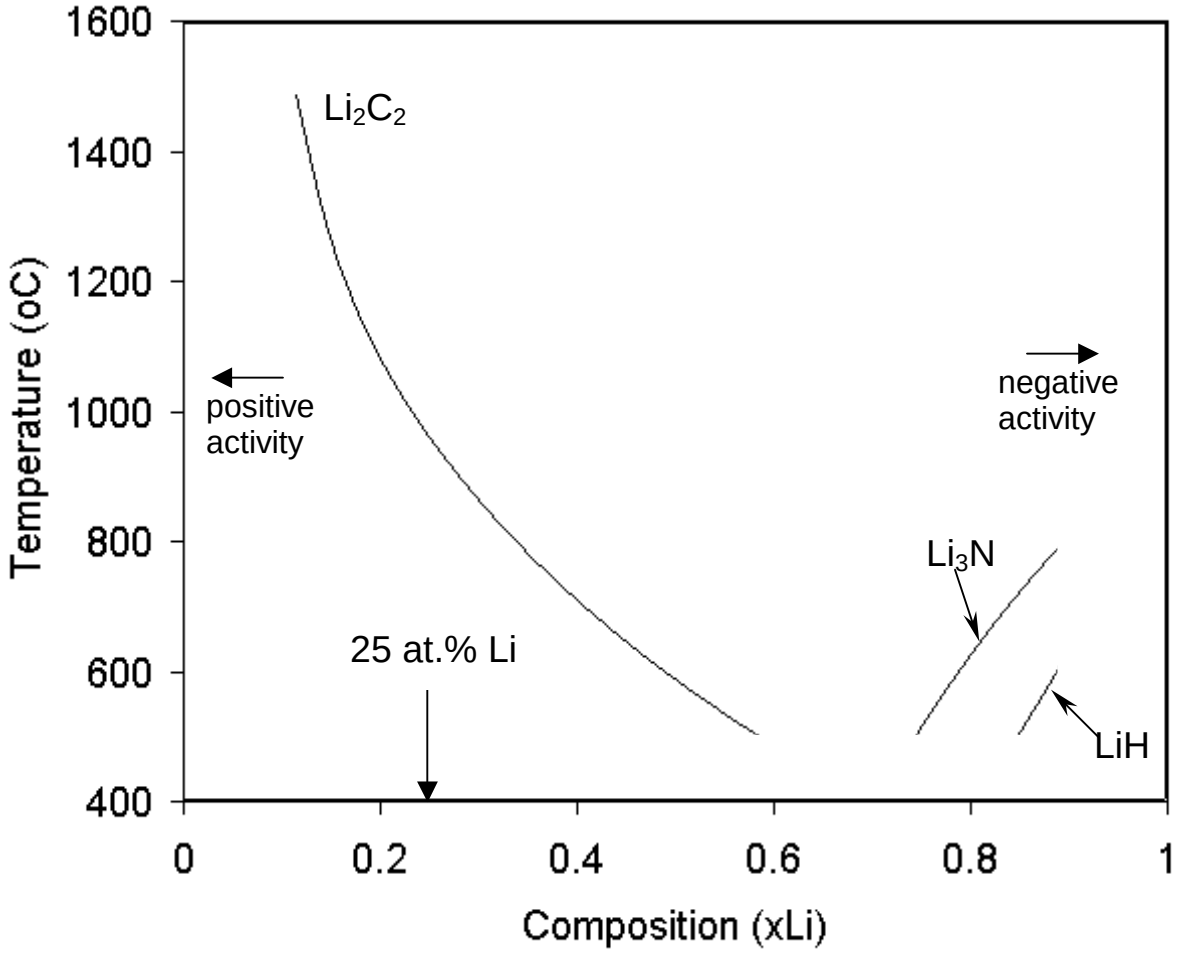


**Figure 14: Limit of formation (*ln $a_i$ = 0; i = C, N, or H*) of $Li_2C_2$, $Li_3N$, and LiH in Sn-Li from Figs. 9, 11, and 13; the corresponding activities are positive to the left of the curves, which indicates dissolution of salts.**

## 5. Thermodynamics of the Interactions of Ceramics with Sn-Li

The chemical viability of coatings in liquid Sn-Li can be assessed by the free energy changes of reaction ($\Delta_r G$). For example, the reduction reaction of an oxide ceramic ($M_xO_y$) in Sn-Li can be expressed the following equation:

$$M_xO_y \xrightarrow{liquid\ Sn-Li} yO(Sn-Li) + xM \qquad (9)$$

and the associated free energy of change of the reaction is expressed as:

$$\Delta_r G = \frac{1}{x}\left\{ y\overline{G_O}(Sn-Li) - \Delta_f G^o(M_xO_y)\right\} \qquad (10)$$

where $\overline{G_O}(Sn-Li)$ is the solute free energy in Sn-Li, in this case of oxygen. Equation 10 represents a relative equilibrium state between the oxygen solute free energy and the Gibbs free energy of the metal oxide formation, which by definition is the thermodynamic driving force $\Delta_r G$. For a smaller $\Delta_f G$ relative to $\overline{G_O}(Sn-Li)$ the oxide is more stable than the oxygen in solution with Sn-Li. This would indicate that the ceramic would be thermodynamically compatible with Sn-Li. In order to evaluate equation 10 for the oxides, nitrides, and carbides the Gibbs free energy of formation and the free energy of the associated solutes needs to be known. The formation energies are tabulated in JANEF Tables [14] but the solute free energies have to be evaluated using solubility data:

$$\begin{aligned} G_O(Sn-Li) &= RT\ln a_O \\ &= RT\ln a_O^* + RT\ln(x_O/x_O^*) \\ &= \Delta_f G^o(Li_2O) - 2\overline{G_{Li}}(Li) + RT\ln(x_O/x_O^*) \end{aligned} \qquad (11)$$

where $a_O^*$ is the oxygen activation at saturation, $x_O$ is the oxygen concentration, and $x_O^*$ is the oxygen concentration at saturation, and $\overline{G}_{Li}$ $(= RT\ln a_{Li})$ is the partial free energy of dissolved lithium. In order to estimate the solubility of the solutes in Sn-Li we rely on the results shown in Figures 5 and 6: of the four lithium salts (LiH, $Li_3N$, $Li_2C_2$ , and $Li_2O$) only $Li_2O$ is sufficiently stable to be formed in Sn-Li, the others decompose to saturated non-metal in solution at $x_{Li} < 0.5$. The solubility of oxygen is very low in *Sn*:at 536, 600, and 700°C the solubility limit are $6\times10^{-6}$, $2\times10^{-4}$, and $6\times10^{-4}$ at. %, respectively [15], and the solubility of oxygen in Pb-Li is also very low [16]. In view of lack of any experimental solubility data it is therefore reasonable to assume that the solubility of oxygen is also very low in Sn-Li. In spite of data, we therefore use the liquid lithium solute solubility expressions [12, 13, 17]:

$$\begin{aligned} \ln x_O &= 1.428 - 6659\ (T/K)^{-1} \\ \ln x_N &= 2.976 - 4832\ (T/K)^{-1} \\ \ln x_C &= -1.100 - 5750\ (T/K)^{-1} \end{aligned} \qquad (12)$$

Because of its low solubility in Sn-Li, oxygen will be maintained at the saturated level regardless of the purification and furthermore, because the lithium salts LiH, $Li_3N$, $Li_2C_2$ decompose readily (at $x_{Li} < 0.65$; T=500ºC), a simplified expression can be derived for the solute free energies:

$$G_O(Sn-Li) = \Delta_f G^o(Li_2O) - 2\overline{G_{Li}}(Li) \qquad (13)$$

Using equation 10 and 13 the free energy of change of reaction for oxide ceramic materials can be evaluated by:

$$\Delta_r G = \frac{1}{x}\left\{ y\left[\Delta_f G^o(Li_2O) - 2\overline{G_{Li}}(Sn-Li)\right] - \Delta_f G^o(M_xO_y)\right\} \qquad (14)$$

### *5. 1 Free energy changes of reaction ($\Delta_r G$) of Ceramics at 773°K*

Figures 15 and 16 show the free energy changes of reaction ($\Delta_r G$) of the oxides listed in Table 7. $Fe_2O_3$, $Cr_2O_3$, and NiO have negative $\Delta_r G$ values in liquid Sn-25Li at 773°K for all compostions of Sn-Li, which indicates that these coatings dissolve. These oxides are thus not compatible with Sn-Li. $B_2O_3$ is stable up to about 20 at. % Li, for compositions with higher lithium content $B_2O_3$ would not be stable. $SiO_2$ and $TiO_2$ are only marginally stable in Sn-25Li at 773°K. $Sc_2O_3$ and $Y_2O_3$ are the most stable oxides.

Figures 17 and 18 depict the free energy changes of reaction of nitrides and carbides, respectively. Based on these estimates, all of the nitrides and carbides are stable in liquid Sn-25Li at 773°K. ZrC and ZrN are the most compatible carbide and nitride in Sn-Li, respectively.

**Table 7: Gibbs free energy of formation of various ceramic materials at 773K [14]..**

| Oxides | $\Delta G_f$(kJ/mol) |
|---|---|
| $Li_2O$ | -497.3 |
| $Al_2O_3$ | -1432.6 |
| $Cr_2O_3$ | -927.7 |
| $Fe_2O_3$ | -617.4 |
| $Sc_2O_3$ | -1679 |
| $Y_2O_3$ | -1678.8 |
| $La_2O_3$ | -1570.4 |
| $Ce_2O_3$ | -1568.4 |
| $B_2O_3$ | -1072.5 |
| $SiO_2$ | -770.3 |
| $TiO_2$ | -802.5 |
| $ZrO_2$ | -952.3 |
| $HfO_2$ | -974.1 |
| $CeO_2$ | -924.9 |
| NiO | -168.9 |
| BeO | -533.1 |
| MgO | -517.4 |
| CaO | -554.1 |
| $LiAlO_2$ | -1024.4 |
| $LiCrO_2$ | -809.2 |
| $Li_2Si_2O_5$ | -2183.5 |
| $Li_2SiO_3$ | -1408.4 |
| $Li_4SiO_4$ | -1963.1 |
| $Li_8SiO_6$ | -2963.9 |

| Nitrides | $\Delta G_f$(kJ/mol) |
|---|---|
| BN | -206.1 |
| AlN | -219.2 |
| Si3N4 | -489.1 |
| TiN | -263.7 |
| ZrN | -291.6 |
| VN | -150.2 |
| TaN | -187.6 |
| CrN | -61.6 |

| Carbides | $\Delta G_f$(kJ/mol) |
|---|---|
| SiC | -73 |
| TiC | -175 |
| ZrC | -189.4 |
| NbC | -134.6 |
| TaC | -141.3 |

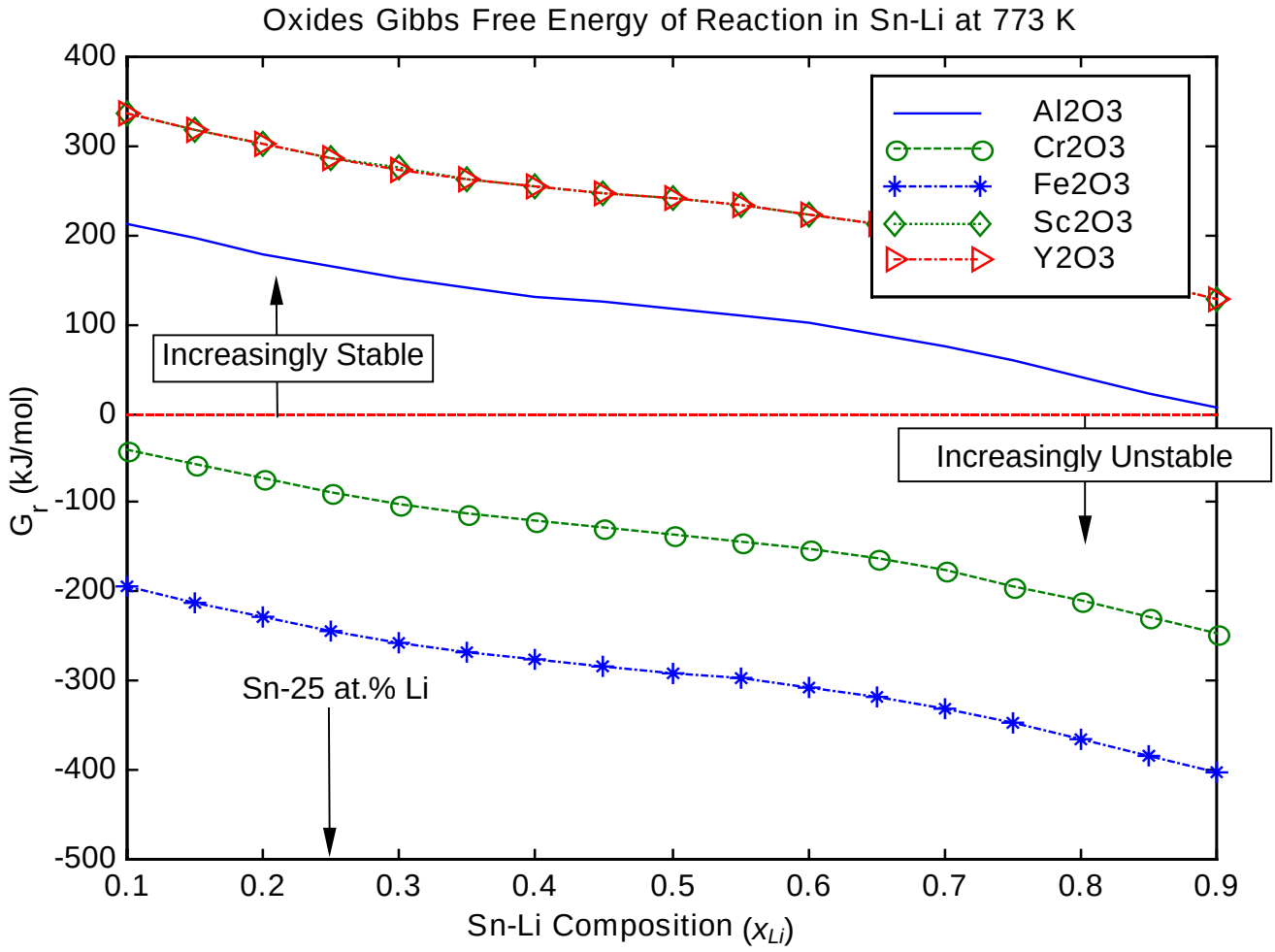


**Figure 15: Free energy changes of reactions (ΔG) of some candidate oxides ceramic materials in liquid Sn-25Li at 773°K.**

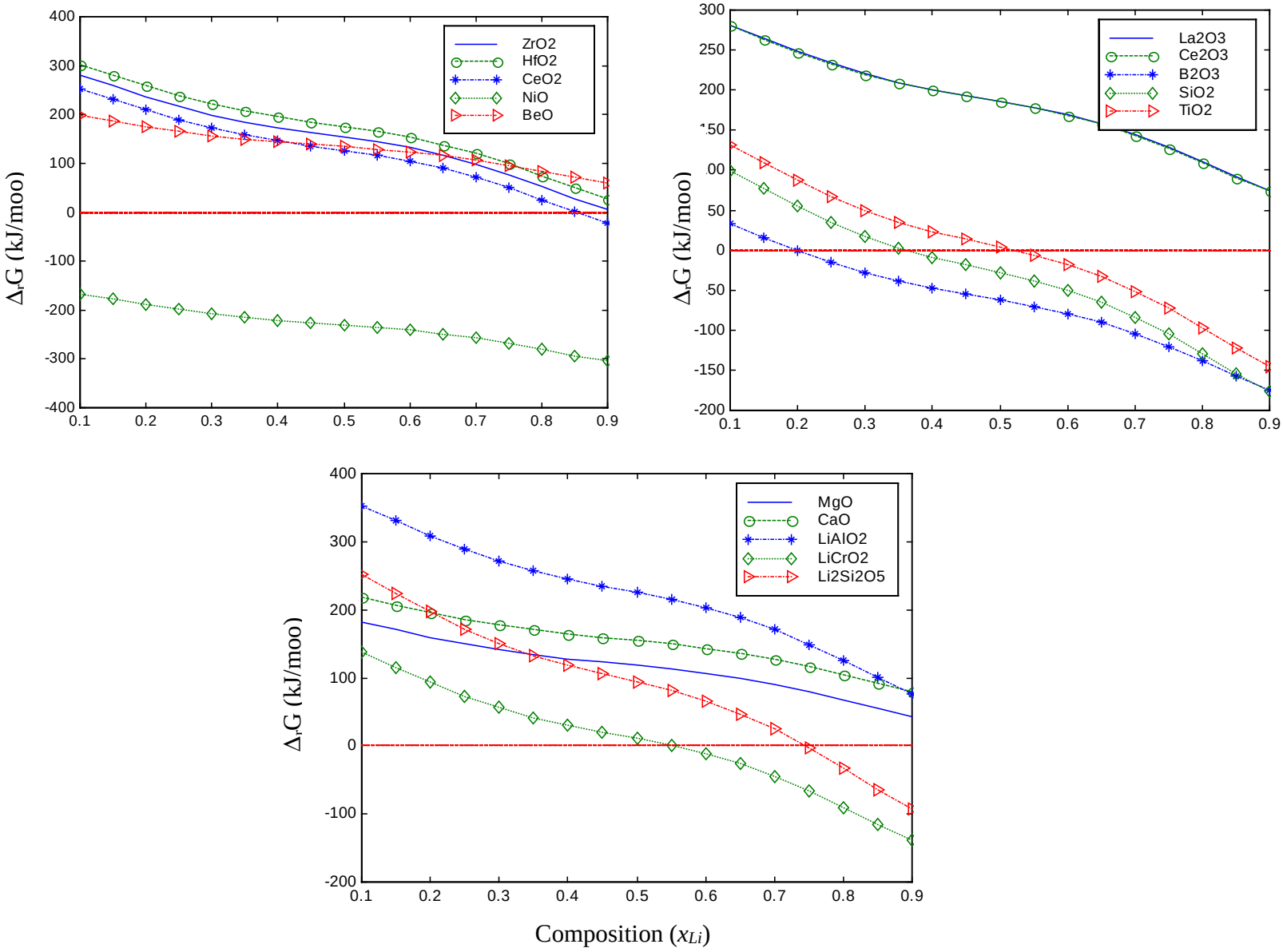


**Figure 16: Free energy changes of reactions of selected oxides in liquid Sn-25Li at 773°K.**

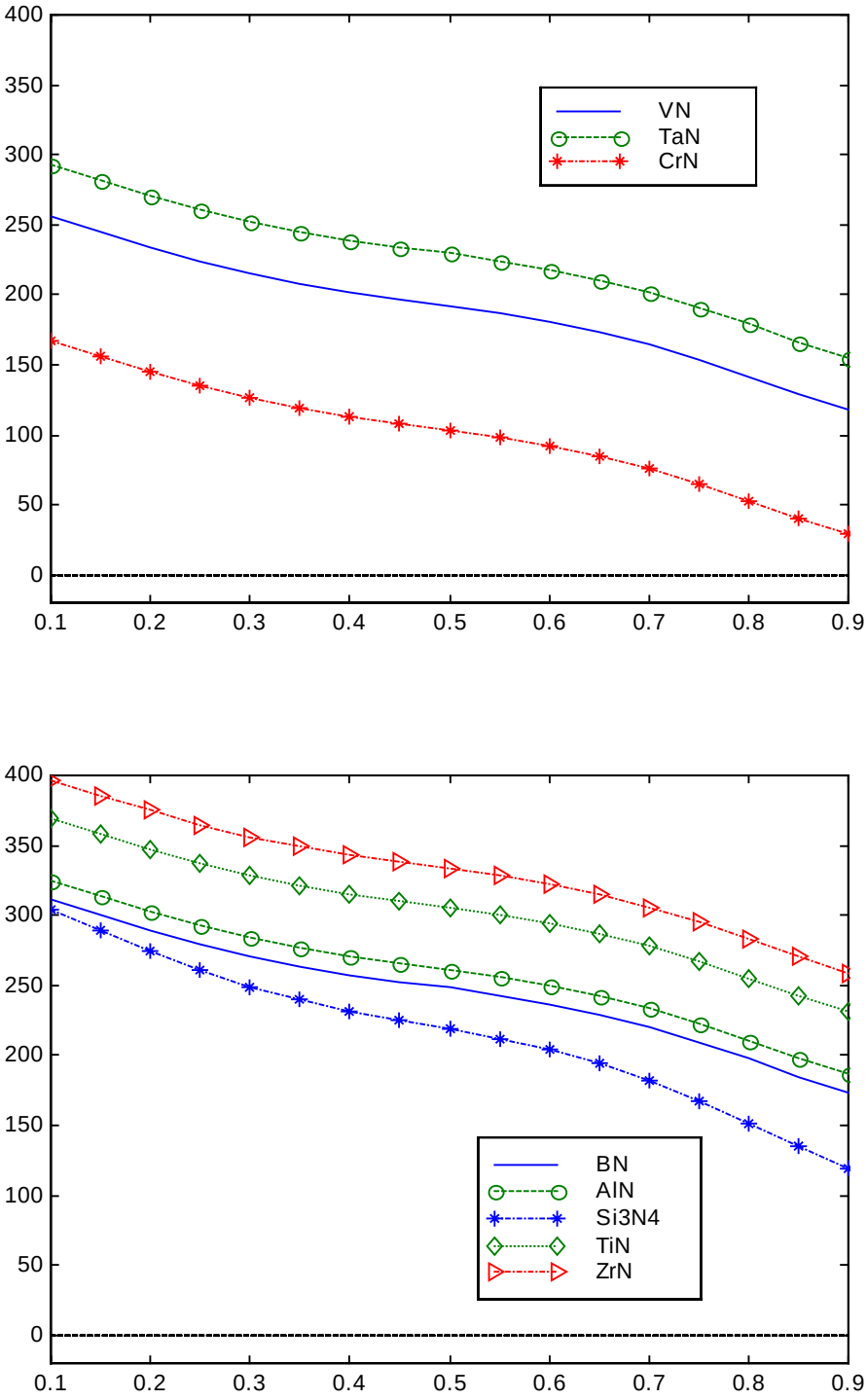


**Figure 17: Free energy changes of reactions of selected nitrides in liquid Sn-25Li at 773°K.**

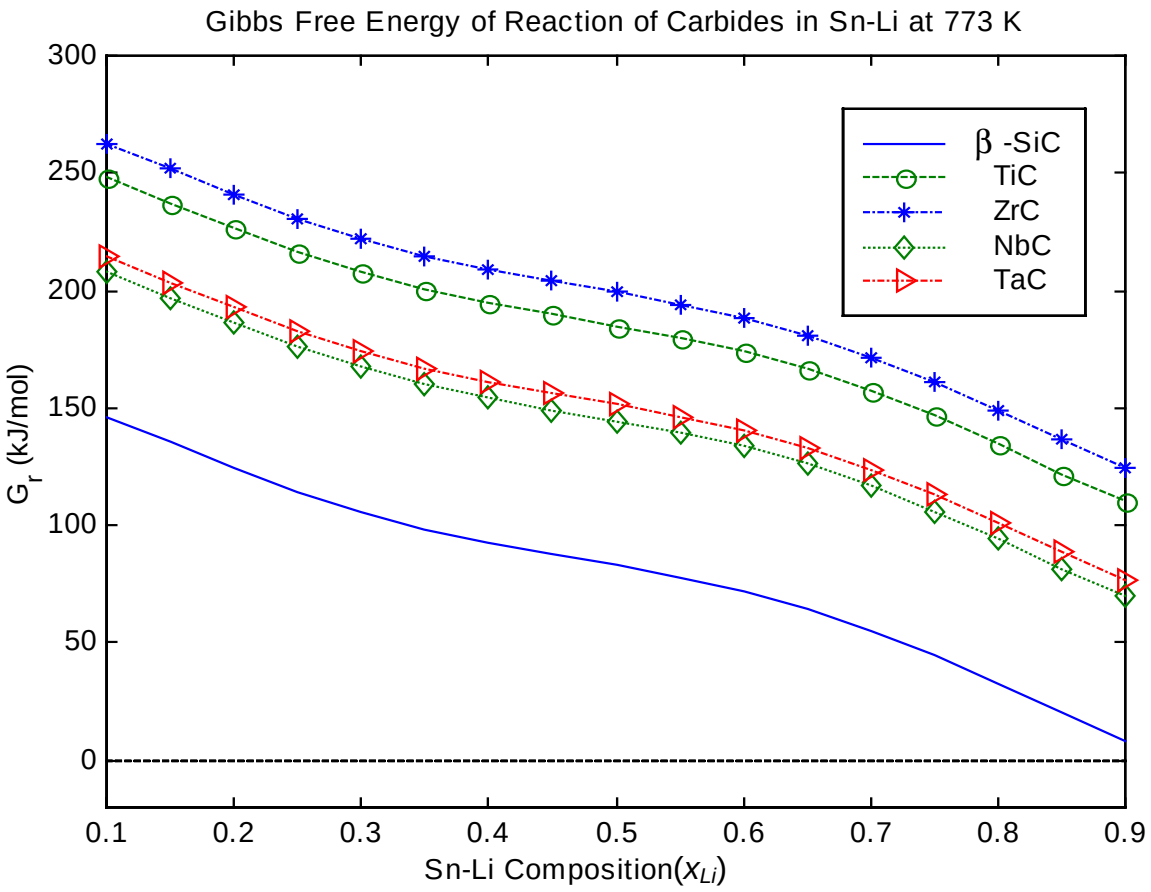


**Figure 18: Free energy changes of reactions of selected carbides in liquid Sn-25Li at 773°K.**

**Table 8: Calculated stability of oxides, nitrides, and carbides in Sn-25Li at 773 K (listed in order of descending stability).**

| Oxides | $\Delta G_r$ |
|---|---|
| | (kJ/mol) |
| $Sc_2O_3$ | 290 |
| $Y_2O_3$ | 290 |
| $LiAlO_2$ | 280 |
| $Al_2O_3$ | 270 |
| $HfO_2$ | 245 |
| $ZrO_2$ | 230 |
| $La_2O_3$ | 225 |
| $Ce_2O_3$ | 224 |
| $CeO_2$ | 295 |
| $Li_2Si_2O_5$ | 290 |
| CaO | 285 |
| BeO | 280 |
| MgO | 255 |
| $TiO_2$ | 75 |
| $LiCrO_2$ | 65 |
| $SiO_2$ | 40 |
| $B_2O_3$ | -15 |
| $Cr_2O_3$ | -100 |
| NiO | -200 |
| $Fe_2O_3$ | -370 |

| Nitrides | $\Delta G_r$ |
|---|---|
| | (kJ/mol) |
| ZrN | 375 |
| TiN | 340 |
| AlN | 290 |
| BN | 280 |
| TaN | 260 |
| Si3N4 | 255 |
| VN | 225 |
| CrN | 130 |

| Carbides | $\Delta G_r$ |
|---|---|
| | (kJ/mol) |
| ZrC | 230 |
| TiC | 215 |
| TaC | 180 |
| NbC | 175 |
| SiC | 115 |

## 6. Compatibility of Ceramic Materials with Sn-Li

The thermodynamic stability of coatings was modeled based on the free energy of changes of reactions between various oxides, nitrides, and carbides. Table 8 summarizes the free energy change of reactions of selected ceramics and Fig. 19 shows a bar-chart representation of their relative stability.

Based on this thermodynamic assessment the nitrides are the most stable ceramics, followed by oxides, and then the carbides. However, among the oxides those of iron and nickel based alloys will probably not be stable. It can be assumed that iron and nickel based alloys will also not be preferred structural materials for Sn-Li.

In summary, based on the solubility of O, N, H, and C in liquid lithium, the following stability results are found for nitride, oxides, and carbide-based coatings in Sn-25Li at 773°K (Fig. 19):

–**Nitrides**:

- At 500°C all of the considered nitrides are stable.
- ZrN is the most stable nitride.

–**Oxides**:

- The most stable oxides are: $Sc_2O_3$ and $Y_2O_3$
- $Fe_2O_3$, NiO, and $Cr_2O_3$ decompose.
- All other considered oxides were found to be stable.
- $TiO_2$ $SiO_2$ marginally stable.
- $B_2O_3$ is unstable at Li-fractions above 0.2.

–**Carbides**

- All carbides including SiC were found to be stable (note: β-SiC is unstable in *pure* Li).
- ZrC is the most stable carbide.

The most stable ceramics are nitrides, followed by oxides, and then by carbides.

## 7. Uncertainties

The thermodynamic model developed here incorporates three assumptions:

1. the activity of lithium was extrapolated using Pb-Li activity data,
2. the solubility of the solutes (O, C, N, H) is based on their solubility in pure lithium, and
3. the Sn-Li contains saturated solution of the solutes.

It may turn out that the lithium activity in Sn is somewhat different from that in Pb-Li. This can only be verified experimentally. The solubility of the solutes in Sn-Li was based on the finding that the solubility of these solutes is very low in pure Sn. Therefore, the solubility of the solutes is dominated by their solubility in lithium.

However, the third assumption may have some significant implications on the actual stability of candidate ceramic coatings. Purification of Sn-Li may be advantages because of radioactivity control, tritium extraction, or bi-metallic loop materials. Therefore, caution must be taken in using the above results for actual system, where cold trapping of solutes may result in significant changes in the thermodynamic behavior of these coatings in liquid Sn-Li.

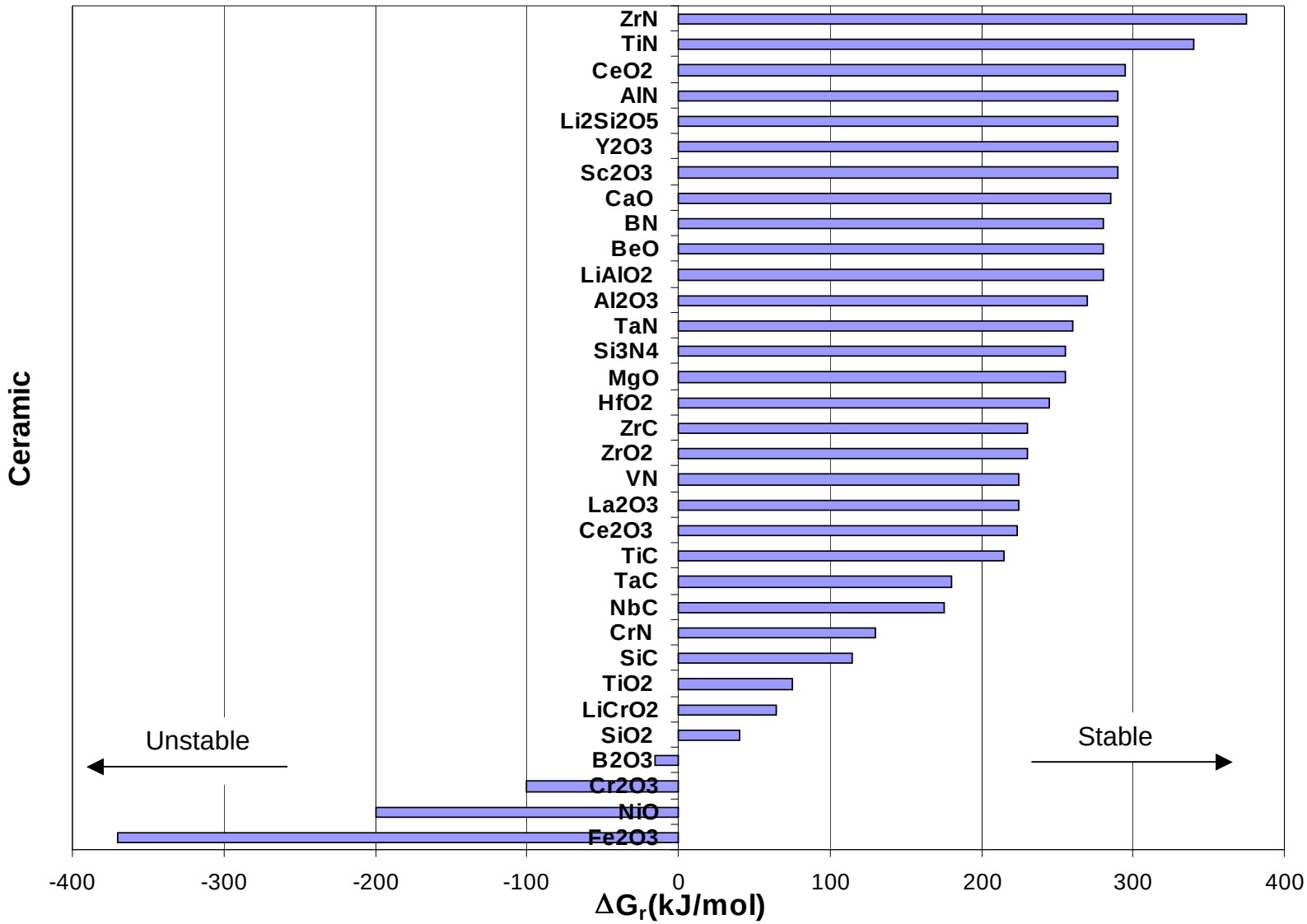


**Figure 19: Estimated $\Delta_r G$ of selected ceramic materials in solute (O, N, C) saturated liquid Sn-25Li at 773°K.**

# 8. References


[1] M. Abdou, et al., "On the Extrapolation of Innovative Concepts for Fusion Chamber Technology," University of California Los Angeles, APEX, Interim Report, Vol. 2, November 1999.

[2] S. Sharafat and N. Ghoniem, "Summary of Thermo-Physical Properties of Sn, and Sn-Li," University of California Los Angeles Report, UCLA-UCMEP-00-31, August 2000; also available on http://www.fusion.ucla.edu/APEX/].

[3] M. Abdou, et al., "On the Extrapolation of Innovative Concepts for Fusion Chamber Technology," University of California Los Angeles, APEX, Interim Report, Vol. 2, November 1999, pp. 8.12.

[4] P. G. Harrison, "Chemistry of Tin," Blackie, Glasgow and London, Chapman and Hall New York, 1989.

[5] M. Abdou, et al., " Blanket Comparison and Selection Study Final Report," Argonne National Laboratory Report, ANL/FPP-84-1, Vol. 2.,1984.

[6] K. K. Kelly, U.S. Bur. Mines Bull. Nr. 383 (1935) 1/132, 105.

[7] B. Schulz, Fusion Eng. Design 14 (1991) 199.

[8] H. A. Davis, J. S. L. Leach, Phys. Chem. Liquids 2 (1970) 1/12, 5.

[9] R. W. Ohse (Ed.) Handbook of Thermodynamic and Transport Properties of Alkali metlas, Inter. Union of Pure and Applied Chemistry Chemical Data Series No. 30. Oxford: Blackwell Scientific Publ., 1985, pp. 987.

[10] D. M. Bailey et al., "Lithium-Tin Phase Relationships between $Li_7Sn_5$ and LiSn," JLCM, 64 (1979)233-240.

[11] K. Natesan and W. E. Ruther, "Fabrication and Properties of a Tin-Lithium Alloy," Fusion Materials, Semiannual Progress Report for the Period Ending Dec. 31, 1999, DOE/ER-0313/27, pp. 203-209.

[12] P. Hubberstey, J. Nucl. Mat. 247 (1997) 208-214.

[13] P. Hubberstey and T. Sample, J. Nucl. Mater. 248(1997) 140-146.

[14] J. Phys. Chem. Ref. Data, Vol. 14, Suppl. 1, 1985.

[15] T. N. Belford Trans. Faraday Soc. 61, 1965.

[16] M. G. Barker, Liquid Metal. Engr. 1984.

[17] P. Hubberstey, A. T. Dadd, P. G. Roberts, in: Liquid Metal System, ed. H. U. Borgstedt, Plenum, New York, 1982. p. 445.